Phys. Status Solidi B **247**, Nos. 11–12, 2909–2914 (2010) / **DOI** 10.1002/pssb.201000555

physica status solidi b
www.pss-b.com
basic solid state physics

Substrate effect on thickness-dependent friction on graphene

Qunyang Li[1], Changgu Lee[2], Robert W. Carpick[1], and James Hone[*,3]

[1] Mechanical Engineering and Applied Mechanics, University of Pennsylvania, Philadelphia, PA 19104, USA
[2] Mechanical Engineering, Sungkyunkwan University, Suwon, Gyeonggi-do 440-746, Korea
[3] Mechanical Engineering, Columbia University, New York, NY 10025, USA

Received 22 June 2010, revised 8 September 2010, accepted 8 September 2010
Published online 22 October 2010

Keywords atomic-scale friction, atomic force microscopy, film thickness, graphene

[*] Corresponding author: e-mail jh2228@columbia.edu, Phone: +1 212 854 6244, Fax: +1 212 854 3304

Using friction force microscopy, we have investigated the frictional behavior of graphene deposited on various substrates as well as over micro-fabricated wells. Both graphene on SiO_2/Si substrates and graphene freely suspended over the wells showed a trend of increasing friction with decreasing number of atomic layers of graphene. However, this trend with thickness was absent for graphene deposited on mica, where the graphene is strongly bonded to the substrate. Measurements together with a mechanics model suggest that mechanical confinement to the substrate plays an important role in the frictional behavior of these atomically thin graphite sheets. Loosely bound or suspended graphene sheets can pucker in the out-of-plane direction due to tip-graphene adhesion. This increases contact area, and also allows further deformation of the graphene when sliding, leading to higher friction. Since thinner samples have lower bending stiffness, the puckering effect and frictional resistance are greater. However, if the graphene is strongly bound to the substrate, the puckering effect will be suppressed and no thickness dependence should be observed. The results can provide potentially useful guidelines in the rational design and use of graphene for nano-mechanical applications, including nano-lubricants and components in micro- and nano-devices.

1 Introduction Graphene has demonstrated excellent properties for electronic, chemical, thermal, and mechanical applications [1]. As a two-dimensional (2D) material consisting of a single layer of atoms, graphene has the high estattainable surface area to volume ratio. Thus, the interaction between a graphene surface and its surroundings is expected to play a more important role in determining the material properties than other bulk-like (3D) materials. For example, graphene sheets supported on SiO_2/Si substrates have shown drastically different carrier mobility [2, 3] and thermal conductivity [4] compared to their suspended counterparts. The morphology of graphene was also recently found to be dependent on the substrates where they were deposited [5–7]. Understanding how graphene interacts with different substrates and how these interactions may affect its mechanical and electronic properties has become a critical step for utilizing graphene reliably. In addition, graphene, as a building unit for a common solid lubricant (graphite), provides an ideal opportunity to study lubrication mechanisms at the nanoscale.

In this work, we systematically explored the frictional properties of graphene sheets exfoliated on various substrates using friction force microscopy. It was found that the frictional properties of these atomically thin graphite layers depend on mechanical confinement from the substrates. For loosely-bound or suspended graphene, friction exhibits a dependence on layer thickness. Measurements at the atomic scale reveal an unusual stick-slip behavior with an initial transient strengthening of the static friction force. However, for graphene strongly bound onto a substrate, the thickness dependence is absent and the frictional properties are indistinguishable from those of bulk graphite. Using a finite element mechanics model, we show that the local puckering due to adhesion with the tip can occur for weakly bound thin sheets, which could account for the observed thickness dependence of friction. Besides the electronic effects previously discovered, this work demonstrates that the substrate can have a profound effect on the mechanical properties of graphene as well as other 2D materials.

2 Friction on supported graphene

2.1 Measurement of graphene on SiO_2/Si substrate Silicon wafers with a top layer of oxide are commonly used as substrates for various graphene devices [8–10] due to facile optical identification of graphene and wide compatibility with conventional fabrication processes. Despite a vast amount of research on this system, how the SiO_2/Si substrate mechanically interacts with graphene and how this interaction affects the mechanical and tribological behavior of graphene has not been well studied. In this work, graphene flakes were deposited onto silicon substrate with thermally grown oxide layers (300 nm) in ambient conditions using micro-mechanical exfoliation [11] and their frictional properties were measured with friction force microscopy (FFM). The substrate was pre-cleaned with a mixture of sulfuric acid and hydrogen peroxide before deposition of graphene to remove organic contamination. After deposition, the thinnest flakes were first identified using optical microscopy; a typical image is shown in Fig. 1(a). These thin flakes have typical lateral dimensions of tens of micrometers, consisting of both thin and thick areas. Their thicknesses were further examined by contact mode atomic force microscopy (AFM) (Park systems XE-100), as schematically shown in Fig. 1(b). The numbers of layers in different areas were independently verified by Raman spectroscopy.

FFM with micrometer-scale lateral scan ranges was performed in an ambient environment (25–50% relative humidity, 20–25°C). Silicon AFM probes (Mikromasch CSC17, nominal tip radius 5–10 nm) were used for the measurements and the normal spring constants (typically around 0.15 N/m) were calibrated using the reference cantilever method [12]. Friction force and topographic images were obtained simultaneously under a fixed normal load of 1 nN. Figure 2(a) shows the topographic image of a thin flake consisting of four distinct regions. The regions labeled 1L, 2L, 3L, and 4L correspond to the areas where the flakes are 1 layer, 2 layers, 3 layers, and 4 layers thick, respectively. The measured thickness per layer closely matches the interlayer spacing of graphene (0.335 nm) in topography.

The friction signal in the forward (left-to-right) direction [Fig. 2(b)] shows a clear trend of increasing friction with decreasing thickness. This trend becomes more apparent

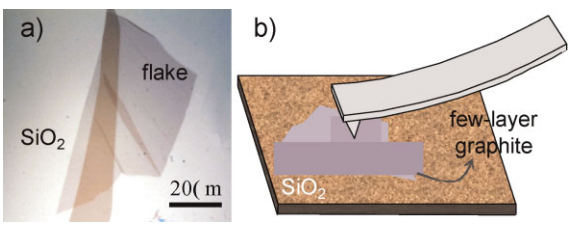

Figure 1 (online colour at: www.pss-b.com) (a) Optical image of exfoliated graphene on SiO_2/Si, showing the dimension and thickness contrast of the flake; (b) a schematic of an AFM tip scanning over a flake containing areas with different thicknesses.

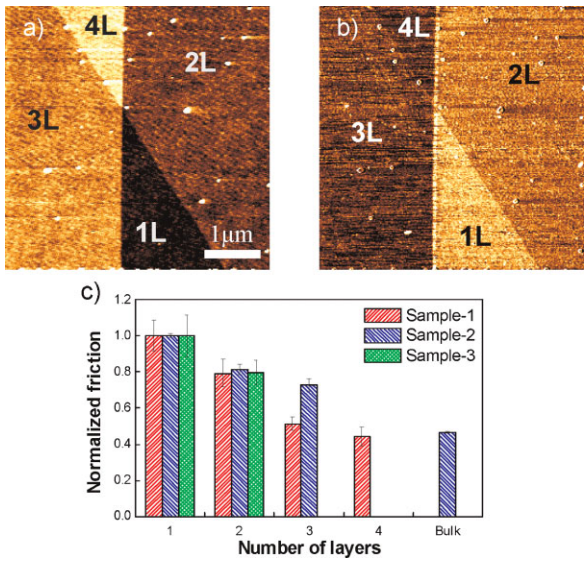

Figure 2 (online colour at: www.pss-b.com) (a) AFM topographic image of the graphene flake, showing four different regions, 1L, 2L, 3L, and 4L, corresponding to areas with 1, 2, 3, and 4 layers of graphene; (b) friction force image of the same area as (a); (c) friction as a function of number of layers for three distinct samples; (a) and (b) were collected on sample-1.

when we plot friction as a function of number of layers in Fig. 2(c). In the figure, three sets of measurements with distinct samples and tips are reported and friction force is calculated by dividing the friction signal difference between the steady-state values in the forward and reverse scans by two. For each set of measurement, we used a same tip while keeping the normal load and scan speed constant. For comparison purposes, the reported friction was normalized to the value measured on 1-layer graphene for each dataset.

For all three datasets, friction decreased monotonically with thickness for 1–5 layers, and leveled off for thicker samples. Compared to 1-layer graphene, friction is ∼20% lower on 2-layer graphene, and 50–60% lower for bulk samples. This observed trend was reproducible for various experimental conditions. It did not depend on scan speed (1–10 μm/s), normal load (1–50 nN) and the tip materials (silicon nitride and diamond). Reducing the humidity from 30 to <5% in dry nitrogen environment led to overall lower friction forces (by ∼20–30%), but the variation of friction with layer thickness was preserved. We also measured the adhesion force between the tips and the samples by performing force-displacement spectroscopy. No appreciable difference in pull-off forces among the areas with different thicknesses could be found within experimental uncertainty.

Nanoscale friction can depend sensitively on the chemistry of the sample. For example, it was found that an adsorbed layer of contaminants can significantly affect friction behavior [13]. Since these sheets are only a few atomic layers thick, they may be more susceptible to the influence of adsorbates. A natural question is how this

possible contamination plays a role in the friction measurements. Moreover, it was also observed that atomic scale friction can be affected by the crystalline orientation of the sample surface [14]. Another important aspect that needs to be examined is how the crystal lattices of exfoliated thin sheets are aligned.

To address these questions, we performed a second set of high resolution measurements by scanning the tip across graphene samples using nanometer-scale scanning distances using an RHK UHV350 AFM in a dry nitrogen purged and subsequently sealed ultrahigh vacuum chamber. The relative humidity inside the chamber was measured to be less than 5% (and is likely 1–2% based on measurements of similar conditions). For these measurements, a silicon probe with a normal spring constant of 0.18 N/m was used (Mikromasch CSC37, calibrated by Sader's method [15]), and the applied normal load was maintained at 4 nN. The friction force was calibrated by a diamagnetic lateral force calibrator [16] and the scan speed was fixed at 40 nm/s for 2 nm scan sizes and at 100 nm/s for 5 nm scan sizes.

The atomic-scale friction results are presented as three columns shown in Figs. 3(a), (b), and (c) for measurements on 1-layer flakes, 4-layer flakes, and bulk graphite. The first row shows line traces of the friction force for 2-nm lateral scans. The tip exhibits clear, periodic stick-slip motion, similar to that previously observed on bulk materials [17]. However, on the 1-layer graphene, the local force at which slip occurs (the static friction force, seen as peaks in the trace) increases in magnitude during as tip continues to slide during each scan. This results in a tilted friction loop as seen clearly in Fig. 3(a). This "strengthening" effect is highlighted by the dotted trend lines in the figure. It is weaker for 4-layer sheet [Fig. 3(b)] and absent for bulk graphite [Fig. 3(c)]. At longer scan lengths of 5 nm, shown in the second row of Fig. 3, the strengthening effect becomes saturated reaching a "steady-state" as the scan proceeds. This suggests that the lateral energy barrier commonly observed in regular stick-slip on bulk materials [17] increases during the initial stage of tip sliding.

During the strengthening portion of the friction loops, the periodicity of slip is in fact slightly elongated along the fast scanning direction. By performing a Fourier transform analysis of the stick-slip friction data, we find that this stretching effect (∼10%) exists only for the strengthening portion of the friction loop, but not for the subsequent "steady-state" portion. Representative examples of raw and filtered friction images on 1-layer, 4-layer, and bulk materials are shown in the third row of Figs. 3(a), (b), and (c), respectively. The structure of the hexagonal-like lattices revealed by the friction images strongly suggests that they are indeed from graphene-like structures, and not from adsorbed contaminants. We can also see that the stretching effect gets weaker as the number of layers increases, and correspondingly, the lattice measured from 4-layer graphene is indistinguishable from that of bulk graphite. By comparing lattice structures, we found that the individual stacked regions of the flake prepared from mechanical exfoliation remain commensurate and share the same orientation to within 0.4°.

Because of the strengthening effect in these nanometer scale measurements, we report the relative frictional energy dissipated per unit cell here instead of average static friction force. This is obtained by first integrating the lateral force over the forward and reverse scan distances and then dividing the result by the number of apparent unit cells scanned. As one can see from Fig. 4, the energy dissipated per unit cell decreases monotonically with an increase in the number of layers, and approaches that measured on bulk materials. The atomic-scale result is qualitatively consistent with the micrometer-scale measurements.

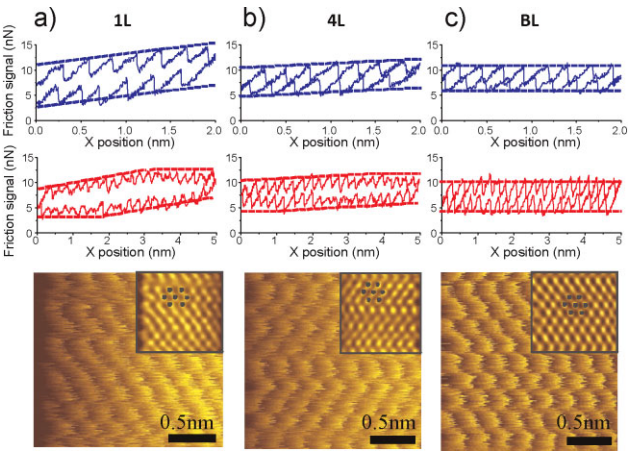

Figure 3 (online colour at: www.pss-b.com) Atomic scale friction results for (a) 1-layer, (b) 4-layer graphene, and (c) bulk graphite. First row: friction loops with short scan length (2 nm). Second row: friction loops with long scan length (5 nm). Third row: stick-slip friction images (insets are low-pass filtered images which more clearly show the underlying lattice structures).

2.2 Measurement of graphene on mica substrates Previously, mica has been used as a substrate to produce ultra-flat graphene samples [7]. The strong

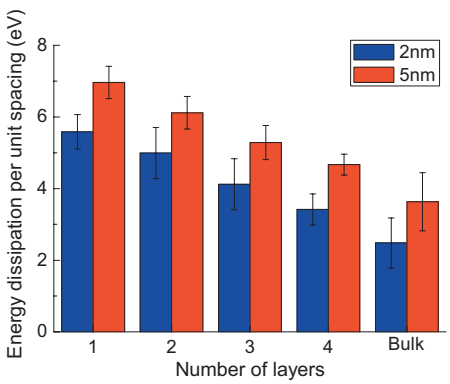

Figure 4 (online colour at: www.pss-b.com) Energy dissipation per unit stick-slip cycle as a function of number of layers.

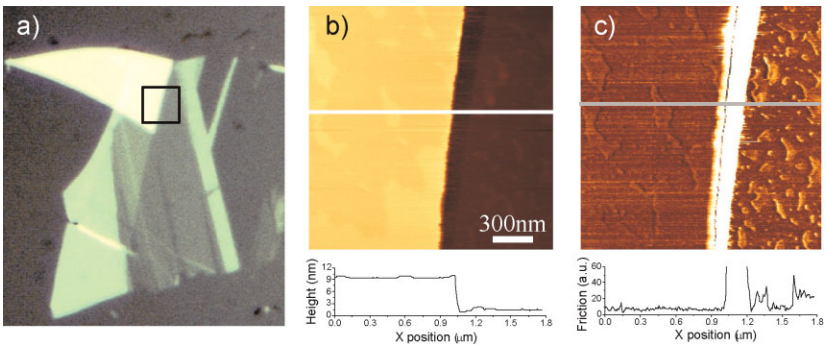

Figure 5 (online colour at: www.pss-b.com) (a) Optical image of graphene on mica. (b) Upper image: AFM topographic image of the square area indicated in (a); lower figure: a line trace showing the height variation across the line in the upper image. (c) Upper image: friction image (in left to right direction) of the same area of (b); lower figure: a line trace showing the friction variation across the line in the upper image.

adhesion between freshly-cleaved muscovite mica surfaces and graphene sheets greatly reduced the surface roughness by suppressing the intrinsic ripples of graphene. How this structural difference in graphene affects its friction behavior, especially the thickness dependence, is a scientifically interesting question to explore. In this work, we also carried out friction measurements on ultra-flat graphene deposited onto mica substrates. Because of the high surface charge and polarity, mica can readily attract water and other adsorbates from the environment upon cleavage; therefore we had to deposit graphene flakes within a few seconds after mica was cleaved. We also tried depositing graphene on mica under dry nitrogen environment inside a glove box. The resultant graphene sample had similar topographic and frictional properties as those prepared in ambient.

Figure 5(a) shows a graphene sample deposited on mica, where 2-layer and thick-layer (9 nm) regions are adjacent to each other. The topographic and friction images of the area marked by the black square box are shown in Figs. 5(b) and (c), respectively. As noticed previously [7], the topographic image [Fig. 5(b)] reveals two distinct regions: atomically flat areas that appear to be in intimate contact with the underlying mica, and slightly (0.2–0.3 nm) elevated "blistered" areas that may be caused by gas or contaminants trapped between the graphene/mica interface. From Fig. 5(c), one can easily see that friction measured on the flat areas is identical for both 2-layer and thick regions, *i.e.*, it exhibits no thickness dependence. However, on the "blistered" areas, friction measured on 2-layer regions is about 2–3 times of that measured on thick-layer, consistent with our previous observations on SiO_2/Si samples. The fact that thickness dependent friction only exists for loosely-adhered "blistered" regions but not on strongly-adhered regions suggests that the interface adhesion between graphene and substrate plays an important role in determining the frictional properties of the thin flakes. Less-confined graphene tends to exhibit the thickness dependent friction behavior.

3 Friction on suspended graphene To further examine the mechanical confinement effect of the substrate on the frictional behavior of graphene, we prepared freely-suspended graphene by depositing it onto SiO_2/Si substrates with arrays of circular wells with a diameter of ~350 nm and a nominal depth of 200 nm [18–20], fabricated by nanoimprint lithography and reactive ion etching. Figure 6(a) shows a graphene flake with 1-layer, 2-layer, and multilayer regions suspended over a well array. Because of the support from the large contacting area and the small size of the wells, the suspended graphene can sustain the deformation without sinking down when the AFM tip scans over it. Figure 6(b) shows a friction image of suspended graphene, where the boundary of the 1-layer and 2-layer regions happens to be laid over a singlewell. The friction measured on the SiO_2/Si supported area, regardless of the thickness of the flake, is indistinguishable from that measured on the freely-suspended area.

4 Discussion and modeling The friction results in Section 2 and 3 clearly demonstrate that friction on graphene flakes critically depends on the interaction between the thin sheets and the substrates. A previous study [5] suggested that graphene exfoliated on SiO_2/Si was partially suspended between higher points of the substrate, and that the intrinsic rippling can still exist for this loosely bound portion of the thin sheet. Due to the same reason of substrate roughness, it is very likely that similar regions of partial suspension also exist for our SiO_2/Si supported graphene. This effect can

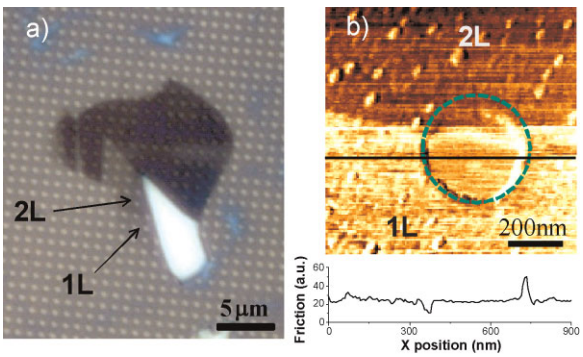

Figure 6 (online colour at: www.pss-b.com) (a) Optical image of a graphene deposited on a substrate with arrays of wells; 1L and 2L are regions with 1-layer and 2-layer graphene; the boundary between 1L and 2L regions happens to run across a micro-fabricated well as can been clearly seen in (b). (b) Upper image: friction image (in left to right direction) measured on the graphene flake suspended over a micro-fabricated well; lower figure: a line trace showing the friction variation across the line in the upper image.

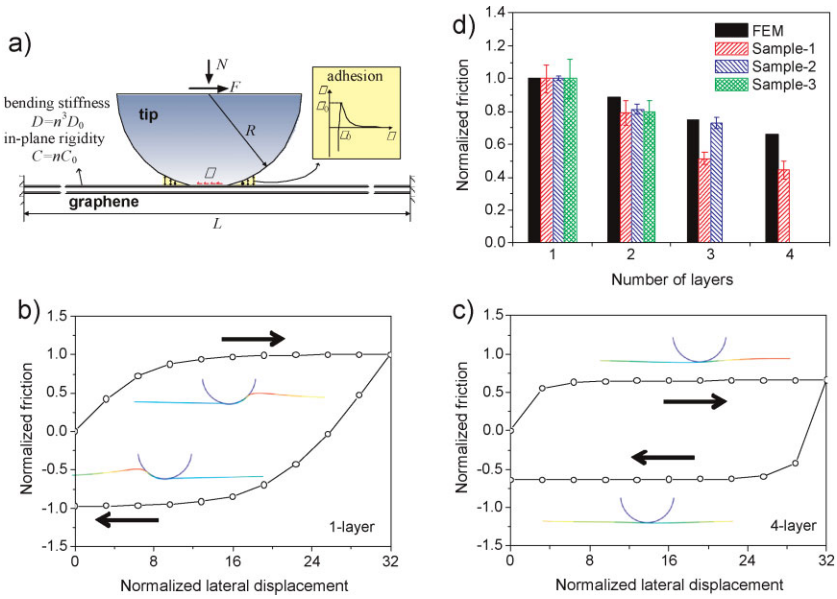

Figure 7 (online colour at: www.pss-b.com) (a) A schematic of the 2D model showing a tip sliding on a suspended graphene thin sheet. (b, c) Calculated friction loops as the tip slides back and forth on a 1-layer and 4-layer graphene, respectively; arrows indicate the sliding direction; insets are local deformation of the thin sheet with the color scale corresponding to the out-of-plane displacement; friction and lateral displacement are normalized by $17.27 \times \overline{\sigma}_0\delta_0$ and δ_0, respectively. (d) Variation of friction *versus* number of layers, including both the FEM simulation result and the micro-scale experimental results; friction forces are normalized to the values for 1-layer graphene.

possibly be further enhanced by third-body species trapped along the interface. This hypothesis is consistent with our observation that friction on SiO_2/Si supported graphene behaves similarly as that on freely-suspended graphene.

When an AFM tip makes contact with such a loosely bound graphene sheet, the sheet can pucker locally due to tip-sheet adhesion. The degree of the puckering and the resulting contact area will depend on the bending stiffness of the sheet: a thinner sheet has lower bending stiffness (proportional to the cube of the thickness according to continuum mechanics) and thereby puckers more, leading to a larger contact area and higher frictional resistance. It is also noted that puckering can also depend on the lateral confinement of the sheet. For example, if the graphene sheet is pinned to the substrate or is under in-plane tension, the puckering effect can be suppressed. In SiO_2/Si supported graphene, the sheet is partly-adhered and has certain slackness due to the intrinsic rippling, both of which enhance the puckering effect. This puckering mechanism may explain why we could observe thickness dependent friction for loosely-bound or freely-suspended graphene. Furthermore, as the tip slides over the loosely bound and slack graphene, the tip can locally displace the graphene with respect to the substrate, which can contribute to the apparent ''stretching'' effect in the lattice-resolved stick-slip measurements that we discussed in Section 2. On the contrary, graphene deposited on mica is believed to be strongly adhered to the substrate with its intrinsic rippling being significantly suppressed, both of which minimize the puckering effect. This explains why no dependence of friction on thickness could be found for graphene deposited on mica.

To quantity the mechanical effect for friction on weakly-confined graphene, we perform a simplified 2D simulation of a tip sliding over a suspended thin sheet using the finite element method (FEM), as shown schematically in Fig. 7(a). The graphene flake is modeled as an elastic plate with a thickness-dependent bending stiffness and in-plane rigidity [21, 22]. In the simulation, n-layer graphene will have bending stiffness $D = n^3D_0$ and in-plane rigidity $C = nC_0$, where D_0, C_0 are bending stiffness and in-plane rigidity for 1-layer graphene [21, 22]. The interaction between the tip and sheet is incorporated by an effective adhesive force derived for graphene based on the Lennard–Jones interaction [23] and a contact-size dependent frictional shear stresses suggested by Müser et al. [24]. The interaction stress ($\overline{\sigma}$) between the graphene and the substrate as a function of inter-surface separation δ follows the form [23]

$$\overline{\sigma} = 3.07\overline{\sigma}_0\left(\frac{1}{(\delta/\delta_0)^4} - \frac{1}{(\delta/\delta_0)^{10}}\right),$$

which is depicted by the inset of Fig. 7(a). The coefficient of friction relating normal and shear stress is μ_0 for the 1-layer contact simulation, and it increases according to $A^{-1/2}\mu_0$ as the contact size gets smaller for thicker sheets, where A is the contact area [24]. In the present simulation, the following parameters were used: $D_0/(\overline{\sigma}_0\delta_0^3) = 180$, $C_0/(\overline{\sigma}_0\delta_0) = 6000$, $R/\delta_0 = 60$, $L/\delta_0 = 4000$, and $\mu_0 = 0.2$.

During the simulation, the tip is brought into contact with the sheet, and then it is slid laterally back and forth while the external normal force (N) is kept at zero and the lateral force (F) is calculated. Figures 7(b) and (c) show the friction loops when the tip is slid back and forth on 1-layer and 4-layer sheets, respectively. Comparing the two friction loops, one can easily see that friction for the thinner sheet is larger than that for the thicker sheet. The local deformation of the thinner sheet [insets of Fig. 7(b)] shows that upon initial contact the thinner sheet puckers up and snaps to the tip due to adhesion. As the tip slides forward, the symmetry of the puckered configuration is broken due to friction, and the thin sheet

piles up in front of the contact edge. On the contrary, the puckering effect and piling up are significantly depressed for the thicker sheet because of its higher bending stiffness, as shown in the insets of Fig. 7(c). The different amount of puckering leads to different contact sizes and therefore different static friction forces. The variation of friction with sheet thickness predicted by FEM simulation is given in Fig. 7(d) together with the micro-scale experimental measurements. The very good qualitative agreement with the experiments suggests that the puckering effect is a feasible mechanism for the thickness-dependent friction behavior. In addition, the development of this piling-up process and its influence on the atomic lattice stick-slip instabilities may also explain the strengthening effect observed in the atomic-scale measurements. We are currently carrying out a systematic study using more elaborate finite element and molecular dynamic simulations to address this issue.

5 Conclusions Using friction force microscopy, we measured friction on graphene samples supported by two solid substrates, SiO_2/Si and muscovite mica, as well as suspended over micro-fabricated wells. Graphene deposited on solid SiO_2/Si substrates exhibited similar frictional behavior as freely-suspended samples, both of which show a trend of increasing friction with decreasing sample thickness. In contrast, the dependence of friction on sample thickness was absent for graphene samples on mica in regions where the graphene was strongly bound to the mica substrate. The experimental results together with the continuum mechanics model suggest that mechanical confinement to the substrate via adhesion has a substantial effect on the frictional behavior of graphene. For loosely-bound and slack graphene samples, friction will depend on the sample thickness. Thinner samples have lower bending stiffness therefore they are more easily puckered in the out-of-plane direction due to tip-graphene adhesion resulting in a higher frictional resistance. However, for strongly bound graphene samples, the puckering effect is suppressed and no thickness dependence is observed. This work clearly demonstrated that a controlled interface between graphene materials and their substrates will be critical for tailoring the tribo-mechanical response in addition to the electronic properties recognized previously.

Acknowledgements We acknowledge support from the NSF under awards NSF/MRSEC (No. DMR-0520020) (R. W. C.), CMMI-0800154 (R. W. C.), CHE-0117752 (J. H.), and CMMI-0927891 (J. H.). We thank C. H. Lui for supplying graphene samples on mica, respectively. We acknowledge helpful discussions with J. Li, M. Müser, and L. Forró.

References

[1] A. K. Geim, Science **324**, 1530 (2009).
[2] K. I. Bolotin, K. J. Sikes, Z. Jiang, M. Klima, G. Fudenberg, J. Hone, P. Kim, and H. L. Stormer, Solid State Commun. **146**, 351 (2008).
[3] J. H. Chen, C. Jang, S. D. Xiao, M. Ishigami, and M. S. Fuhrer, Nature Nanotechnol. **3**, 206 (2008).
[4] J. H. Seol, I. Jo, A. L. Moore, L. Lindsay, Z. H. Aitken, M. T. Pettes, X. S. Li, Z. Yao, R. Huang, D. Broido, N. Mingo, R. S. Ruoff, and L. Shi, Science **328**, 213 (2010).
[5] V. Geringer, M. Liebmann, T. Echtermeyer, S. Runte, M. Schmidt, R. Ruckamp, M. C. Lemme, and M. Morgenstern, Phys. Rev. Lett. **102**, 4 (2009).
[6] M. Ishigami, J. H. Chen, W. G. Cullen, M. S. Fuhrer, and E. D. Williams, Nano Lett. **7**, 1643 (2007).
[7] C. H. Lui, L. Liu, K. F. Mak, G. W. Flynn, and T. F. Heinz, Nature **462**, 339 (2009).
[8] K. S. Novoselov, A. K. Geim, S. V. Morozov, D. Jiang, Y. Zhang, S. V. Dubonos, I. V. Grigorieva, and A. A. Firsov, Science **306**, 666 (2004).
[9] Y. Zhang, Y.-W. Tan, H. L. Stormer, and P. Kim, Nature **438**, 201 (2005).
[10] J. S. Bunch, A. M. van der Zande, S. S. Verbridge, I. W. Frank, D. M. Tanenbaum, J. M. Parpia, H. G. Craighead, and P. L. McEuen, Science **315**, 490 (2007).
[11] K. S. Novoselov, D. Jiang, F. Schedin, T. J. Booth, V. V. Khotkevich, S. V. Morozov, and A. K. Geim, Proc. Natl. Acad. Sci. USA **102**, 10451 (2005).
[12] M. Tortonese and M. Kirk, Micromachining and Imaging, Vol. 3009 (SPIE, San Jose, CA, USA, 1997), p. 53.
[13] G. He, M. H. Muser, and M. O. Robbins, Science **284**, 1650 (1999).
[14] M. Dienwiebel, G. S. Verhoeven, N. Pradeep, J. W. M. Frenken, J. A. Heimberg, and H. W. Zandbergen, Phys. Rev. Lett. **92**, 4 (2004).
[15] J. E. Sader, J. W. M. Chon, and P. Mulvaney, Rev. Sci. Instrum. **70**, 3967 (1999).
[16] Q. Li, K. S. Kim, and A. Rydberg, Rev. Sci. Instrum. **77**, 13 (2006).
[17] C. M. Mate, G. M. McClelland, R. Erlandsson, and S. Chiang, Phys. Rev. Lett. **59**, 1942 (1987).
[18] C. Lee, X. Wei, J. W. Kysar, and J. Hone, Science **321**, 385 (2008).
[19] C. Lee, X. Wei, Q. Li, R. Carpick, J. W. Kysar, and J. Hone, Phys. Status Solidi B **246**, 2562 (2009).
[20] C. Lee, Q. Li, W. Kalb, X.-Z. Liu, H. Berger, R. W. Carpick, and J. Hone, Science **328**, 76 (2010).
[21] B. I. Yakobson, C. J. Brabec, and J. Bernholc, Phys. Rev. Lett. **76**, 2511 (1996).
[22] M.-F. Yu, O. Lourie, M. J. Dyer, K. Moloni, T. F. Kelly, and R. S. Ruoff, Science **287**, 637 (2000).
[23] L. Y. Jiang, Y. Huang, H. Jiang, G. Ravichandran, H. Gao, K. C. Hwang, and B. Liu, J. Mech. Phys. Solids **54**, 2436 (2006).
[24] M. H. Müser, L. Wenning, and M. O. Robbins, Phys. Rev. Lett. **86**, 1295 (2001).

